ACS APPLIED MATERIALS & INTERFACES

Biological and Medical Applications of Materials and Interfaces

Self-Powered Biosensors Using Various Light Sources in Daily Life Environments: Integration of *p-n* Heterojunction Photodetectors and Colorimetric Reactions for Biomolecule Detection

Kihyeun Kim, Hyeonghun Kim, Hyungjun Jang, Jiyoon Park, Gun Young Jung, and Min-Gon Kim

ACS Appl. Mater. Interfaces, **Just Accepted Manuscript** • DOI: 10.1021/acsami.8b13457 • Publication Date (Web): 30 Oct 2018

Just Accepted

ACS Publications

is published by the American Chemical Society. 1155 Sixteenth Street N.W., Washington, DC 20036

Self-Powered Biosensors Using Various Light Sources in Daily Life Environments: Integration of *p-n* Heterojunction Photodetectors and Colorimetric Reactions for Biomolecule Detection

Kihyeun Kim[1], *Hyeonghun Kim*[2], *Hyungjun Jang*[1], *Jiyoon Park*[2], *Gun-Young Jung*[2*] *and Min-Gon Kim*[1*]

[1]Department of Chemistry, Gwangju Institute of Science and Technology (GIST), Gwangju 61005, Republic of Korea

[2]School of Materials Science and Engineering, Gwangju Institute of Science and Technology (GIST), Gwangju 61005, South Korea

*Email: mkim@gist.ac.kr (Min-Gon Kim), gyjung@gist.ac.kr (Gun-Young Jung)

KEYWORDS: self-powered biosensor, photodetector, *p-n* heterojunction, colorimetric reaction, glucose detection

ABSTRACT

Electronic biosensors operating without power supply are high in demand owing to increasing interest in point-of-care (POC) coupled with portable and wearable electronic devices for smart healthcare services. Although self-powered electronic sensors have emerged with the promise of resolving the energy supply problems, achieving sufficient sensitivity to targets in real samples is highly challenging because of the matrix effect caused by electroactive species. In this study, we developed a self-powered biosensor platform by combining *n*-IGZO/*p*-Si heterojunction photodetectors and physically separated colorimetric reactions. The self-powered biosensors were applied to glucose detection in real human samples using light sources from daily life environments such as fluorescent light and sunlight. The sensors showed high sensitivity and stability from 0.01 mg ml^{-1} to 10 mg ml^{-1} of glucose in human saliva and urine without matrix effect from the electroactive species in real samples. In addition, a small change in glucose concentration in human serum was distinguishable with resolution 0.01 mg ml^{-1}. Notably, these results were obtained using well-developed and widely used materials like Si and IGZO with simple deposition techniques. Moreover, this self-powered biosensing platform can be universally applied for detection of all biomolecules being detected by colorimetric assays. To the best of our knowledge, the present paper is the first report on such self-powered biosensors, which could be a promising candidate for future POC biosensors integrated with portable and wearable electronic devices.

INTRODUCTION

Biomolecule detection using electronic sensors is of interest in clinical analysis because of their high sensitivity, portability, and adaptability to smart electronic devices.[1-3] These merits extend their application to point-of-care (POC) integrated with electronic devices systems for seamless health monitoring at any place and anytime, which leads to successful treatment of diseases.[4,5] A major challenge to developing such sensor systems is the use of battery power owing to its limited lifetime, recharging inconvenience, and insufficient battery level to operate the integrated sensor systems.[6-9] Hence, with the objective of reducing the power consumption of electronic sensor systems, many studies have been conducted based on emerging 2D materials that have high mobility and the structural design of nanomaterial-based devices.[10-12] However, despite advancements in nanomaterials and electronic devices for low-power consumption, there is an increasing demand for sensor systems that operate without batteries in order to enhance adaptability and portability for future POC biosensors.

Self-powered biosensors have attracted considerable attention as a potential future POC sensor platform coupled with smart electronic devices because they can operate using energy from the local environment without the need for batteries.[7-9,13,14] Since the first report of self-powered biosensors based on electrochemical reactions by Willner *et al*. in 2001, self-powered biosensors have been mainly explored based on an electrochemical sensing platform to detect various target molecules such as glucose and cholesterol.[15-19] Such self-powered biosensors are operated by electricity from oxidation and reduction reactions at the anode and cathode, respectively. Those self-powered sensing platforms, however, suffer from decreased performance due to matrix effects caused by electroactive species in physiological samples such as urine, saliva, and serum, which consist of ions, uric acid, enzymes, *etc*.[19,20] Although photo-induced electrochemical biosensors

for self-powered systems have been recently studied to further enhance sensitivity and reliability, this approach inevitably results in additional electricity for restricted light generators (e.g., UV lamp and LED) in order to excite electrons to induce photoelectrochemical reactions at electrodes.[21-24] Moreover, it is still difficult to avoid the matrix effect because of the direct contact between reactants and electrodes. Thus, it remains a challenge to fulfill the requirements of sensitivity, stability, and operation without power supplies for future POC biosensor systems.

In this paper, we report on self-powered photodetectors with colorimetric reactions for a highly practical and universal self-powered biosensing platform, which is operated by any visible light sources in daily life environments such as fluorescent light and sunlight, which makes the whole sensor system free from the need for a power supply, and widens its practical uses under any weather conditions. The self-powered photodetector is simply fabricated by depositing *n*-IGZO thin film onto *p*-Si wafer, thereby forming a *p*-*n* heterojunction. In polydimethylsiloxane (PDMS) molds precisely located on the upper side of the IGZO/Si photodetectors, a physically separated enzyme-based colorimetric reaction occurs. Further, reduction in the photocurrent of the IGZO/Si photodetectors occurs as a result of production of colored products due to target injection, which block the light reaching the IGZO/Si detectors, and facilitates the quantification of glucose levels. The physical isolation of the detectors and the colorimetric reaction leads to high and stable sensitivity towards glucose in real human samples, without the matrix effect. In addition, this self-powered biosensor platform is capable of detecting all targets being detected by colorimetric assays. Hence, application of such self-powered biosensors could be expanded to POC biosensors and smart healthcare systems.

RESULTS AND DISCUSSION

Figure 1a illustrates the structural concept of self-powered biosensors composed of self-powered photodetectors and PDMS vessels for colorimetric reaction. Colorimetric reaction is commonly used for biomolecule detection, which changes in color when a target is injected. The reaction occurs in the PDMS vessel for determination of the glucose concentration, which is located at the upper side of the self-powered photodetectors, coinciding with the exact light pathway. Both the PDMS and detectors are fixed at the customized sensor case made by a 3D printer (Figure S1). This structure has two main advantages in practical use: (i) avoidance of the matrix effect in real sample detection owing to physical isolation between the reaction and detection parts; (ii) the PDMS vessel is disposable, whereas IGZO/Si photodetectors are reusable. Figure 1b illustrates the detection mechanism of self-powered photodetectors with colorimetric reaction. Injection of glucose into the PDMS vessel containing glucose oxidase (GOx), N, N-bis (4-sulfobutyl)-3,5-dimethylaniline (MADB), 4-aminoantipyrine (4-AAP), and peroxidase induces the change in the color of the solution due to oxidized condensation products blocking the light. Thus, the intensity of light reaching the self-powered photodetectors is reduced, which causes a decrease in the devices' photocurrent. The photocurrent change enables quantitative determination of the concentration of glucose. Colorimetric reaction with enzyme is a well-known method for glucose detection, leading to a change in the solution color.[25,26] The reaction pathway for glucose in this case is given by Equations (1) and (2) and is shown in Figure 1c.

$$\text{Glucose} + O_2 \xrightarrow{\text{glucose oxidase}} \text{gluconic acid} + H_2O_2 \quad (1)$$

$$\text{MADB} + H_2O_2 + \text{4-AAP} \xrightarrow{\text{peroxidase}} \text{colored product (630 nm)} + H_2O \quad (2)$$

As a result of glucose detection by colorimetric reaction in a 96-well plate, the higher concentration of glucose induced the deeper-colored products, as shown in Figure 1d. Absorption spectra of the colored products in the 96-well plate are shown in Figure S2, and the peak is located at 630 nm.

The self-powered photodetectors were fabricated by depositing *n*-IGZO thin film onto single crystal *p*-Si substrate (a lightly doped *p*-type silicon wafer) by forming a *p*-*n* heterojunction. The roles of Si and IGZO are light absorption under visible light irradiation and carrier transport layers, respectively. This combination of Si and IGZO has two main advantages. Firstly, single crystal Si is highly efficient in the absorption of visible light owing to its extremely low defect level and low bandgap (1.1 eV); whereas, the bandgap of IGZO is 3.1 eV where visible light penetrates. This ensures that light sources can be easily chosen in daily life environments, as there is no need for power consumption for light irradiation. Secondly, in general, the IGZO thin film as a *n*-type semiconductor shows high mobility, thus it is suitable to be used as a carrier transport layer. The fabrication process of the devices is described in Figure S3a.

A depletion region was formed in the entire IGZO layer because of the relative thinness of 30 nm (Figure S3b), which is important for obtaining high photosensitivity for the self-powered photodetectors. This is because the internal potential in IGZO minimizes recombination of the electron-hole pair during collection of carriers reaching the electrodes. The silver finger electrode, which can form ohmic contact with IGZO, was deposited using a metal shadow mask on IGZO/Si. A detailed band diagram of Ag, *n*-IGZO, and *p*-Si is described in Figure S3c. The self-powered photodetectors at zero-voltage bias show a highly stable photocurrent with a fast response and recovery time (within 0.1 s for both) under a 650 nm laser (Figure S3d). The fast response and recovery of the devices without hysteresis stem from the single crystal silicon, which absorbs the light.

The photocurrent of self-powered photodetectors was measured after injection of various glucose concentrations in DI water under laser and fluorescent light (Figure 2). The sensitivity of the devices was defined as the percentage change in photocurrent due to the colorimetric reaction,

$$\text{Sensitivity (\%)} = [(I_i - I_f) / I_i] \times 100 \quad (3)$$

where I_i is the initial photocurrent before glucose injection and I_f is the photocurrent after glucose injection. In the case of I_f, photocurrent measurement started 30 s after glucose injection. In Figure 2a, photocurrent is measured under a 650 nm laser (0.1 mW), which is matched with the absorption peak of reactant, at different concentrations of glucose in DI water ranging from 0.01 mg ml^{-1} to 10 mg ml^{-1}. Photocurrent is dramatically reduced by increasing the concentration of glucose, and its sensitivities are 0, 5.6, 57.2, 85.2, and 99.4% for the concentration of glucose in DI water of 0, 0.01, 0.1, 1, and 10 mg ml^{-1}, respectively. To measure the photocurrent of self-powered photodetectors using fluorescent light in daily life environments, the sensor system was placed on a table in our laboratory (Figure S4a), and the experiment was conducted only at night to eliminate the effect of sunlight. The sensitivities of the devices decreased relatively under fluorescent light compared with laser illumination; specifically, 4.5, 36.4, 58.4, and 79.0% for the concentration of glucose in DI water of 0, 0.01, 0.1, 1, and 10 mg ml^{-1}, respectively (Figure 2b). The reduced sensitivities are due to the emission spectrum of the fluorescent light containing mainly 550 nm and 610 nm (Figure S4b), which is not fully absorbed by the colored product having an absorption peak at 630 nm.

Figure 3 shows the sensitivity dependence on intensity and the incident angle of the fluorescent light on the self-powered photodetectors. The light intensity and angle are controlled

by turning on and off three switches in our laboratory. Three different light conditions were chosen to characterize the sensitivity of the self-powered biosensors: (1) only one fluorescent light was turned on; it was located on just the upper side of the sensors (Figure 3a); (2) the other two diagonally-located fluorescent lights were turned on, and the light obliquely reached the sensors (Figure 3b); (3) just one diagonally-located fluorescent light was turned on (Figure 3c). In all three cases, the self-powered biosensors show a similar sensitivity towards 0–10 mg ml^{-1} glucose in DI water regardless of the intensity and incident angle of the fluorescent light (Figures 3d–3f). Thus, it is possible to reliably measure the glucose concentration using the self-powered biosensors under a static light source, such as laser and fluorescent light.

Two identical self-powered photodetectors and PDMS vessels were used to determine glucose concentration under sunlight, as shown in Figure S5, because the intensity of sunlight changes from moment to moment. The sensor system with two devices was placed in a sunny area of the laboratory. Photocurrents of the two devices equally changed in accordance with the sunlight intensity, as shown in Figure 4a; thus, one device was used as a control sample for calibration and the other for detection of glucose. The solution contained in the PDMS vessel for the control sample was composed of the colored reagent, GOx, peroxidase, and 4-AAP, but not the color development reagent, MADB. The sensitivity was calculated as the percentage change between control and detection devices:

$$\text{Sensitivity (\%)} = [(I_c - I_d) / I_c] \times 100 \quad (4)$$

where I_c is the photocurrent of the control sample and I_d is the photocurrent of the detection sample after glucose injection. In the case of I_d, photocurrent measurement started 30 s after glucose

injection. The values of both I_c and I_d for sensitivity calculation were chosen at exactly the same time. Figure 4b shows that the sensitivities in the site of sunshine are 3.4, 29.5, 45.7, and 54.7% for the concentration of glucose in DI water of 0, 0.01, 0.1, 1, and 10 mg ml^{-1}, respectively. (Note: The five different graphs were merged in Figure 4b to clarify the different sensitivities towards different glucose concentrations; each graph is differently colored and there are breaks between them.) The self-powered biosensors can successively detect target molecules even under sunlight of varying intensities at each moment. Although there is a decrease in sensitivity under sunlight owing to its wide light spectrum, photocurrent changes are still adequately sensitive to detect glucose in DI water ranging from 0.01 mg ml^{-1} to 10 mg ml^{-1}. In addition, it is confirmed that the light intensity dependence of sensitivity towards glucose is not observed under sunlight, which changes in terms of intensity from moment to moment (Figure S6). A repeated experiment for each condition was carried out, and the results are shown in Figure 4c. A comparison of sensitivities toward glucose in DI water under three different light sources shows a similar tendency to concentration of glucose.

Sensing performance towards glucose in real samples was investigated by spiking glucose into real human saliva and urine. The photocurrent measurement procedure and sensitivity calculation were the same as in the cases of detection of glucose in DI water. The final concentrations of saliva and urine were 10 times diluted when they were injected into PDMS molds. The sensitivities of glucose in saliva and urine are shown in Figures 5a and 5b, respectively. Glucose in non-spiked saliva and urine was not detected by the self-powered biosensors under any of the three light sources. Detectable sensitivity was initially observed when saliva and urine were spiked with 0.01 mg ml^{-1} of glucose (final concentration). Considering that the final glucose concentrations in saliva and urine are 0.0008 mg ml^{-1} and 0.0011 mg ml^{-1}, respectively (Table

S1), the amount of glucose in the two real samples is much too low to be detected by the self-powered biosensors. Nevertheless, the sensors show a similar sensitivity and the same tendency compared to glucose in DI water. Thus, it is confirmed that there is negligible matrix effect on the self-powered biosensors caused by inorganic salts and organic compounds in real samples, which is due to the physically separated reaction part and detection part in the sensor system.

Among the glucose levels in the real human samples, the serum glucose level is the key factor in real clinical diagnosis.[27,28] Thus, the self-powered biosensors were used to measure glucose concentration in human serum. The purchased human serum was analyzed using a clinical analyzer (Hitachi 7020) and found to contain 0.98 mg ml^{-1} of glucose (Table S1), which is within the range of normal fasting serum glucose levels, while increased risk for diabetes is regarded over 1.25 mg ml^{-1}.[29] Therefore, glucose in non-spiked and spiked (final concentrations of spiked glucose: 0.01 mg ml^{-1}, 0.02 mg ml^{-1}, 0.04 mg ml^{-1}, 0.06 mg ml^{-1}, 0.08 mg ml^{-1}, and 0.1 mg ml^{-1}) human serum was measured using the self-powered biosensors under fluorescent light and sunlight illumination, as shown in Figure 6. The sensitivities to non-spiked and 0.01, 0.02, 0.04, 0.06, 0.08, and 0.1 mg ml^{-1} spiked human serum were 29, 32, 34, 35, 37, 39, and 41%, respectively for under fluorescent light (Figure 6a), and 13, 15, 18, 20, 22, 24, and 26%, respectively for under sunlight (Figure 6b). (Note: The eight different graphs were merged in Figure 6b to clarify the different sensitivities towards different glucose concentrations; each graph was differently colored and there are breaks between them.) Hence, precise analysis of the serum glucose level was possible using self-powered biosensors, which shows great potential for real clinical diagnosis of glucose.

Finally, the performance of the self-powered photodetectors with colorimetric reaction was compared with previously reported self-powered glucose sensors. Our self-powered biosensors exhibited superior performance towards real human saliva and urine with no power consumption

compared with the others as shown in Table 1.[15,22,23,30-34] It is noteworthy that this superior sensitivity is obtained using commercially available materials (*n*-IGZO and *p*-Si) and simple deposition techniques. Moreover, any previously reported colorimetric assays can be applied to our self-powered biosensors.[35-40] This makes the sensors more attractive for a universal POC biosensor platform integrated with smart electronic devices.

CONCLUSIONS

In this paper, we demonstrated self-powered biosensors by introducing the colorimetric reaction to *n*-IGZO/*p*-Si heterojunction photodetectors, thereby operating with no power consumption by detector or light sources by employing light available in daily life environments. Such self-powered biosensors are highly suitable to the biosensing platforms for smart and wearable electronic devices, which suffer from battery limitations. Moreover, the physically separated reaction part and the detection part in the self-powered biosensors are responsible for high sensitivity and stable monitoring of glucose in real samples without the matrix effect, which allowing detection from 0.01 to 10 mg ml^{-1} of glucose in saliva and urine with a fast-diagnostic time (30 s) under laser, fluorescent light, and sunlight. In addition, in the detection of serum glucose levels, increases in glucose concentration of 0.01 mg ml^{-1} steps were distinguished, which is sufficient to diagnose hyperglycemia. Notably, this high sensitivity was obtained using commonly utilized materials and simple deposition techniques. Moreover, the proposed self-powered biosensing platform is highly adaptable for detecting any disease detectable by colorimetric assays simply by changing the reactant in disposable PDMS vessels. Hence, the self-powered biosensors presented in this paper can set the foundation for notable development of POC

biosensors combined with smart electronic device technologies, leading to smart healthcare systems.

EXPERIMENTAL SECTION

Materials. D-(+)-glucose (BioXtra, ≥ 99.5) and 4-aminoantipyrine (4-AAP, reagent grade) were obtained from Sigma Aldrich. Glucose oxidase (GOx, GLO-201, 100 U mg^{-1}) and peroxidase (PEO-301, 110 U mg^{-1}) were purchased from Toyobo Co., Ltd. (OSK, Japan). N, N-bis (4-sulfobutyl)-3,5-dimethylaniline, disodium salt (MADB) (M_w: 423.46, ≥ 99.5) were purchased from Dojindo Molecular Technologies, Inc. (Tokyo, Japan). Phosphate buffered saline (PBS, pH 7.4) was purchased from Biosesang (Seongnam, South Korea). Pooled normal human urine and pooled normal human saliva were purchased from Innovative Research (Novi, USA). Human serum (from human male AB plasma, USA origin, sterile-filtered, H4522) was purchased from Sigma Aldrich.

Fabrication and characterization of self-powered photodetectors. *N*-type InGaZnO thin films were deposited on *p*-type silicon substrate using DC sputtering, as previously reported.[41] Composition of the IGZO target was In_2O_3:Ga_2O_3:ZnO = 1:1:1 (atomic ratio), and the thicknesses of the deposited-IGZO thin films were 30 nm at a pressure of 3×10^{-6} mbar with 1% O_2 partial pressure. 30 nm of silver thin film as the top electrode was then deposited through a metal shadow mask using e-beam evaporator on the IGZO/Si substrate. Copper tape was attached to the bottom of the IGZO/Si substrate using silver paste as the bottom electrode. Photocurrent was measured using chronoamperometry analysis (Compactstat; Ivium technologies, Netherlands) by applying 0 V under laser, fluorescent light, and sunlight illumination.

Light sources. Laser (maximum power: 20 mW; power was controlled using an ND filter) was purchased from LS Korea, Korea. The fluorescent light used was from conventional fluorescent lamps in the ceiling of our laboratory, and was two meters above the measurement table, as shown in Figure S4a. Real sunlight was used by placing self-powered biosensors in a sunny place in our laboratory (with the fluorescent light turned off).

Preparation of sensing system for measurement. Cases for sensing measurement were fabricated using a 3D printer (Ultimaker 3) and the materials were polylactic acid. The cases were composed of two parts. The bottom part was needed for placing the self-powered photodetectors. The top part having rectangular hole was used to place the PDMS mold. The size of each part is written in Figure S1. The PDMS mold was prepared as a reaction vessel for colorimetric reaction, and the volume of the PDMS vessel was 15 mm × 5 mm × 2 mm (length × width × height). To assemble the sensing cases, firstly, self-powered photodetectors were placed on the bottom part of the case, and the wiring process was performed on each top and bottom electrode using copper wire and silver paste. Secondly, the top part was placed on the bottom part, and PDMS mold was placed on the top part of the case. In the case of two-sample detection, the cases were designed as a dual room for two samples, as shown in Figure S5.

Glucose detection measurement under various light sources. Glucose sensing experiments were performed in the previously fabricated sensor cases with IGZO/Si photodetectors and the PDMS vessels. Firstly, optimized solution for glucose detection composed of PBS (pH 6.0), 0.05 M 4-AAP, 0.05 M MADB, 50 U ml^{-1} peroxidase, and 50 U ml^{-1} glucose oxidase at a ratio of 6:1:1:1 was prepared. Into the PDMS vessel, 180 µl of the solution was poured, and the vessel was partially covered with glass. The glass cover was employed to fully cover the area where light penetrates and reaches the self-powered photodetectors. This was done to avoid

the side effect of any unintentional change in the intensity of the light reaching the detectors caused by morphology of the solution. Twenty microliters (20 μl) of various concentrations of spiked glucose (final concentration: 0, 0.01, 0.1, 1, 10 mg ml^{-1}) in DI water, real human urine, and real human saliva were then injected into the PDMS vessel; as a result, real samples were finally diluted 10 times. Regarding detection of glucose in human serum, non-spiked and spiked (final concentrations of the spiked glucose: 0.01 mg ml^{-1}, 0.02 mg ml^{-1}, 0.04 mg ml^{-1}, 0.06 mg ml^{-1}, 0.08 mg ml^{-1}, and 0.1 mg ml^{-1}) human serum were used. Photocurrent was measured using chronoamperometry analysis (Compactstat; Ivium technologies, Netherlands); in the case of glucose detection, the measurement started 30 s after injection of glucose in all results. All the photocurrent measurements of Ag/IGZO/Si photodetectors were performed at zero voltage bias. With regard to illumination of sunlight, two identical self-powered photodetectors (one for calibration; the other for detection) were used, and the solution in the PDMS vessel for calibration sample consisted of 4-AAP, GOx, and peroxidase except for MADB. To use sunlight for glucose detection, the two identical self-powered biosensors were placed near the window of the laboratory, in sunlight.

Analysis of glucose concentration in real human samples. Glucose concentrations in real human saliva, urine, and serum were analyzed using Hitachi 7020 Clinical Analyzer (Hitachi High-Technologies Corporation, Japan).

AUTHOR INFORMATION

Corresponding Author

*Min-Gon Kim (mkim@gist.ac.kr)

*Gun-Young Jung (gyjung@gist.ac.kr)

ORCID

Min-Gon Kim: 0000-0002-3525-0048

Author Contributions

M.-G. K., G-.Y. J. and K. K. designed and developed the self-powered biosensor platform. K. K. performed measurement and analyzed the results in this paper. H. K. and H. J. fabricated the photodetectors and sensor cases, respectively. J. P. measured photocurrent of the self-powered photodetectors under solar simulator. The draft of this paper was written by all the authors: K. K., H. K., H. J., J. P., G-.Y. J. and, M-.G. K.

Notes

The authors declare no competing financial interest.

ACKNOWLEDGMENT

This work was financially supported by grants from the Global Research Laboratory (GRL) Program (NRF-2013K1A1A2A02050616) and the Mid-career Researcher Program (NRF-2017R1A2B3010816) through a National Research Foundation grant funded by the Ministry of Science, ICT, and Future Planning. G.Y. Jung was supported by the Pioneer Research Center Program (NRF-2016M3C1A3908893) through the National Research Foundation of Korea (NRF) funded by the Ministry of Education.

Supporting Information. The supporting information is available free of charge via the Internet at http://pubs.acs.org.

The following sections are included: A detailed size of the 3D printed senor case and fabrication process of the proposed *p*-*n* heterojunction photodetectors. Analysis of the IGZO thin film using scanning electron microscope (SEM). A band diagram of Ag, IGZO, and Si. Photocurrent of *p*-*n* heterojunction photodetectors. Absorption spectrum of product from the colorimetric reaction. Digital image of fluorescent light in laboratory and its emission spectrum. Raw data of photocurrent measurement for glucose detection under sunlight. Glucose concentrations in human saliva, urine, and serum. Photocurrent measurement of the self-powered photodetectors under AM 1.5G illumination**.**

REFERENCES

(1) Joo, S.; Brown, R. B. Chemical Sensors with Integrated Electronics. *Chem*. *Rev*. **2008**, *108*, 638–651.

(2) Luo, X.; Davis, J. J. Electrical Biosensors and the Label Free Detection of Protein Disease Biomarkers. *Chem. Soc. Rev.* **2013**, *42*, 5944–5962.

(3) Torsi, L.; Magliulo, M.; Manoli, K.; Palazzo, G. Organic Field-Effect Transistor Sensors: A Tutorial Review. *Chem. Soc. Rev.* **2013**, *42*, 8612–8628.

(4) Islam, S. M. R.; Kwak, D.; Kabir, MD. H.; Hossain, M.; Kwak, K.-S. The Internet of Things for Health Care: A Comprehensive Survey. *IEEE Access* **2015**, *3*, 678–708.

(5) McRae, M. P.; Simmons, G.; Wong J.; McDevitt, J. T. Programmable Bio-Nanochip Platform: A Point-of-Care Biosensor System with the Capacity to Learn. *Accounts Chem*. *Res*. **2016**, *49*, 1359–1368.

(6) Wang, K.; Wang, Y.; Sun, Y.; Guo, S.; Wu, J. Green Industrial Internet of Things Architecture: An Energy-Efficient Perspective. *IEEE Commun. Mag.* **2016**, *54*, 48–54.

(7) Haight, R.; Haensch, W.; Friedman, D. Solar-Powering the Internet of Things. *Science* **2016**, *353*, 124–125.

(8) Wang, Z. L. Self-Powered Nanosensors and Nanosystems. *Adv. Mater.* **2012**, *24*, 280–285.

(9) Wang, Z. L.; Chen, J.; Lin, L. Progress in Triboelectric Nanogenerators as a New Energy Technology and Self-Powered Sensors. *Energy Environ. Sci.* **2015**, *8*, 2250–2282.

(10) Sarkar, D.; Liu, W.; Xie, X.; Anselmo, A. C.; Mitragotri, S.; Banerjee, K. MoS_2 Field-Effect Transistor for Next-Generation Label-Free Biosensors. *ACS Nano* **2014**, *8*, 3992–4003

(11) McAlpine, M. C.; Ahmad, H.; Wang, D.; Heath, J. R. Highly Ordered Nanowire Arrays on Plastic Substrates for Ultrasensitive Flexible Chemical Sensors. *Nat. Mater.* **2007**, *6*, 379–384.

(12) Han, J.-W.; Rim, T.; Baek, C.-K.; Meyyappan, M. Chemical Gated Field Effect Transistor by Hybrid Integration of One-Dimensional Silicon Nanowire and Two-Dimensional Tin Oxide Thin Film for Low Power Gas Sensor. *ACS Appl. Mater. Interfaces* **2015**, *7*, 21263–21269.

(13) Wang, Z. L. Toward Self-Powered Sensor Networks. *Nano Today* **2010**, *5*, 512–514.

(14) Ha, M.; Park, J.; Lee, Y.; Ko, H. Triboelectric Generators and Sensors for Self-Powered Wearable Electronics. *ACS Nano* **2015**, *9*, 3421–3427.

(15) Katz, E.; Bückmann, A. F.; Willner, I. Self-Powered Enzyme-Based Biosensors. *J. Am. Chem. Soc.* **2001**, *123*, 10752–10753.

(16) Gai, P.-P.; Ji, Y.-S.; Wang, W.-J.; Song, R.-B.; Zhu, C.; Chen, Y.; Zhang, J.-R.; Zhu, J.-J. Ultrasensitive Self-Powered Cytosensor. *Nano Energy* **2016**, *19*, 541–549.

(17) Sekretaryova, A. N.; Beni, V.; Eriksson, M.; Karyakin, A. A.; Turner, A. P. F.; Vagin, M. Y. Cholesterol Self-Powered Biosensor. *Anal. Chem.* **2014**, *86*, 9540–9547.

(18) Hickey, D. P.; Reid, R. C.; Milton, R. D.; Minteer, S. D. A Self-Powered Amperometric Lactate Biosensor Based on Lactate Oxidase Immobilized in Dimethylferrocene-Modified LPEI. *Biosens*. *Bioelectron*. **2016**, *77*, 26–31.

(19) Grattieri, M.; Minteer, S. D. Self-Powered Biosensors. *ACS Sens.* **2018**, *3*, 44–53.

(20) Yogeswaran, U.; Chen, S.-M. A Review on the Electrochemical Sensors and Biosensors Composed of Nanowires as Sensing Material. *Sensors* **2008**, *8*, 290–313.

(21) Zhao, K.; Yan, X.; Gu, Y.; Kang, Z.; Bai, Z.; Cao, S.; Liu, Y.; Zhang, X.; Zhang, Y. Self-Powered Photoelectrochemical Biosensor Based on CdS/RGO/ZnO Nanowire Array Heterostructure. *Small* **2016**, *12*, 245–251.

(22) Tian, J.; Zhu, H.; Chen, J.; Zheng, X.; Duan, H.; Pu, K.; Chen, P. Cobalt Phosphide Double-Shelled Nanocages: Broadband Light-Harvesting Nanostructures for Efficient Photothermal Therapy and Self-Powered Photoelectrochemical Biosensing. *Small* **2017**, *13*, 1700798.

(23) Dai, W.-X.; Zhang, L.; Zhao, W.-W.; Yu, X.-D.; Xu, J.-J.; Chen, H.-Y. Hybrid PbS Quantum Dot/Nanoporous NiO Film Nanostructure: Preparation, Characterization, and Application for a Self-Powered Cathodic Photoelectrochemical Biosensor. *Anal. Chem.* **2017**, *89*, 8070–8078.

(24) Soares da Silva, F. G.; Cerqueira dos Santos, G. K.; Yotsumoto Neto, S.; de Cássia Silva Luz, R.; Damos, F. S. Self-Powered Sensor for Tannic Acid Exploiting Visible LED Light as Excitation Source. *Electrochim. Acta* **2018**, *274*, 67–73.

(25) Wang, J. Electrochemical Glucose Biosensors. *Chem. Rev.* **2008**, *108*, 814–825.

(26) DuBois, M.; Gilles, K. A.; Hamilton, J. K.; Rebers, P. A.; Smith, F. Colorimetric Method for Determination of Sugars and Related Substances. *Anal. Chem.* **1956**, *28*, 350–356.

(27) Jee, S. H.; Ohrr, H.; Sull, J. W.; Yun, J. E.; Ji, M.; Samet, J. M. Fasting Serum Glucose Level and Cancer Risk in Korean Men and Women. *JAMA* **2005**, 293, 194–202.

(28) Liu, M.; Liu, R.; Chen, W. Graphene Wrapped Cu_2O Nanocubes: Non-Enzymatic Electrochemical Sensors for the Detection of Glucose and Hydrogen Peroxide with Enhanced Stability. *Biosens*. *Bioelectron.* **2013**, *45*, 206–212.

(29) American Diabetes Association. Diagnosis and Classification of Diabetes Mellitus. *Diabetes Care* **2014**, *37*, S81–S90.

(30) Liu, Z.; Cho, B.; Ouyang, T.; Feldman, B. Miniature Amperometric Self-Powered Continuous Glucose Sensor with Linear Response. *Anal. Chem.* **2012**, *84*, 3403–3409.

(31) Cheng, H.; Yu, P.; Lu, X.; Lin, Y.; Ohsaka, T.; Mao, L. Biofuel Cell-Based Self-Powered Biogenerators for Online Continuous Monitoring of Neurochemicals in Rat Brain. *Analyst* **2013**, *138*, 179–185.

(32) Valdés-Ramírez, G.; Li, Y.-C.; Kim, J.; Jia, W.; Bandodkar, A. J.; Nuñez-Flores, R.; Miller, P. R.; Wu, S.-Y.; Narayan, R.; Windmiller, J. R.; Polsky R.; Wang J. Microneedle-Based Self-Powered Glucose Sensor. *Electrochem. Commun.* **2014**, *47*, 58–62.

(33) Fischer, C.; Fraiwan, A.; Choi, S. A 3D Paper-Based Enzymatic Fuel Cell for Self-Powered, Low-Cost Glucose Monitoring. *Biosens. and Bioelectron.* **2016**, *79*, 193–197.

(34) Jeerapan, I.; Sempionatto, J. R.; Pavinatto, A.; You, J.-M.; Wang, J. Stretchable Biofuel Cells as Wearable Textile-Based Self-Powered Sensors. *J. Mater. Chem. A* **2016**, *4*, 18342–18353.

(35) Byun, J.-Y.; Shin, Y.-B.; Kim, D.-M.; Kim, M.-G. A Colorimetric Homogeneous Immunoassay System for the C-Reactive Protein. *Analyst* **2013**, *138*, 1538.

(36) Shim, W.-B.; Song, J.-E.; Mun, H.; Chung, D.-H.; Kim, M.-G. Rapid Colorimetric Detection of Salmonella Typhimuriumusing a Selective Filtration Technique Combined with Antibody–Magnetic Nanoparticle Nanocomposites. *Anal. Bioanal. Chem.* **2014**, *406*, 859–866.

(37) Shim, W.-B.; Lee, C.-W.; Kim, M.-G.; Chung, D.-H. An Antibody–Magnetic Nanoparticle Conjugatebased Selective Filtration Method for the Rapid Colorimetric Detection of Listeria Monocytogenes. *Anal*. *Methods*, **2014**, *6*, 9129.

(38) Seok, Y.; Byun, J.-Y.; Mun, H.; Kim, M.-G. Colorimetric Detection of PCR Products of DNA from Pathogenic Bacterial Targets Based on a Simultaneously Amplified DNAzyme. *Microchim. Acta* **2014**, *181*, 1965–1971.

(39) Batule, B. S.; Kim, S. U.; Mun, H.; Choi, C.; Shim, W.-B.; Kim, M.-G. Colorimetric Detection of Norovirus in Oyster Samples through DNAzyme as a Signaling Probe. *J. Agric. Food Chem.* **2018**, *66*, 3003–3008.

(40) Kim, S. U.; Batule, B. S.; Mun, H.; Shim, W.-B.; Kim, M.-G. Ultrasensitive Colorimetric Detection of Salmonella Enterica Typhimurium on Lettuce Leaves by HRPzyme-Integrated Polymerase Chain Reaction. *Food Control* **2018**, *84*, 522–528.

(41) Kumaresan, Y.; Pak, Y.; Lim, N.; kim, Y.; Park, M.-J.; Yoon, S.-M.; Youn, H.-M.; Lee, H.; Lee, B. H.; Jung, G. Y. Highly Bendable In-Ga-ZnO Thin Film Transistors by Using a Thermally Stable Organic Dielectric Layer. *Sci. Rep.* **2016**, *6,* 37764.

Table of Contents

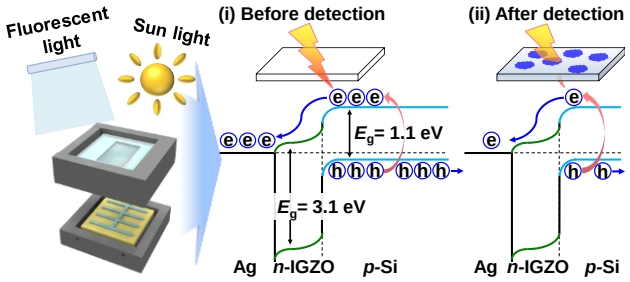

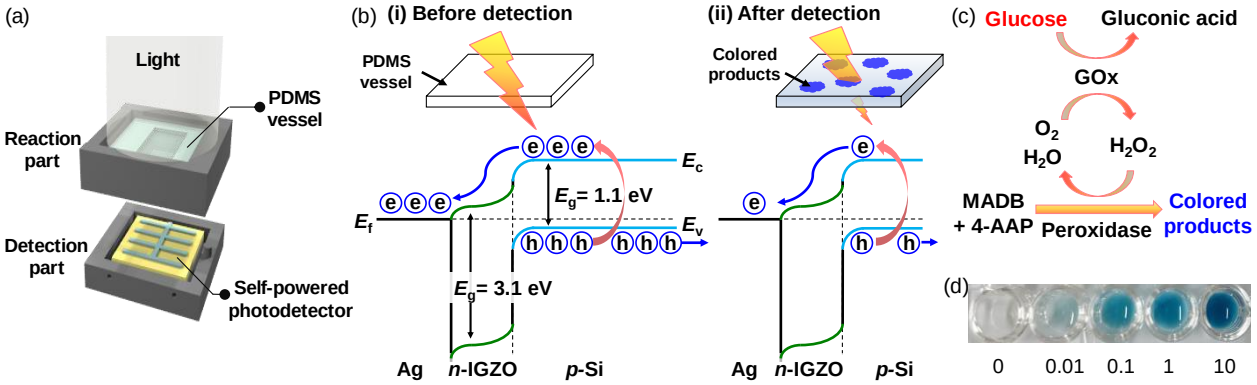

Figure 1. (a) Schematic illustration showing the structure of the self-powered biosensors composed of the vertically located sensing part of PDMS and the detector part of *n*-IGZO/*p*-Si photodetectors. (b) Detection mechanism of the self-powered biosensors. (c) Principle of colorimetric reaction. (d) Digital image of the result of colorimetric reaction of 0, 0.01, 0.1, 1, and 10 mg ml^{-1} glucose in a 96-well plate starting from the left.

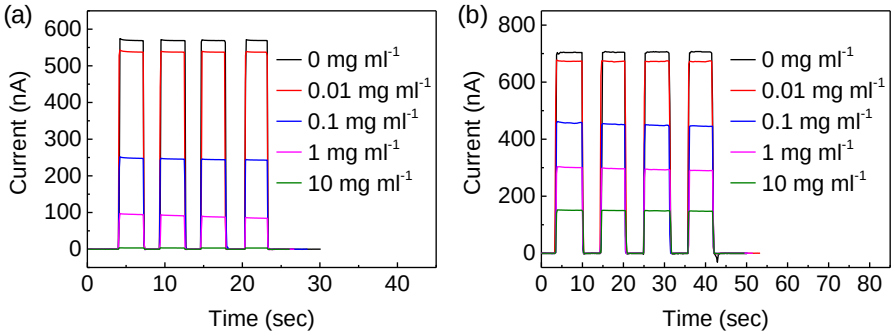

Figure 2. Detection performance of the self-powered biosensors towards glucose in DI water. Photocurrent changes induced by colorimetric reaction depending on the concentration of glucose under (a) 650 nm laser 0.1 mW, and (b) fluorescent light.

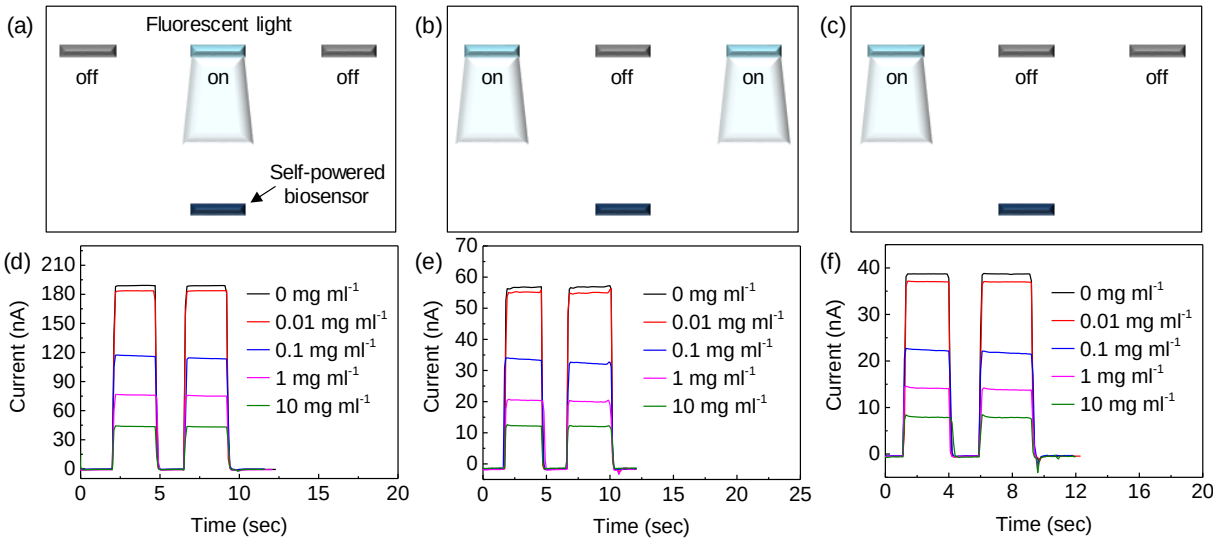

Figure 3. Glucose (in DI water) detection by measuring photocurrent under different intensities and angles of fluorescent light. The light angle and intensity were controlled by turning on and off of three switches of the fluorescent light. (a) Direct incident light (one switch on). Oblique incident light with (b) two switches on and (c) one switch on. Photocurrents under each light condition are (d), (e), and (f) for (a), (b), and (c), respectively.

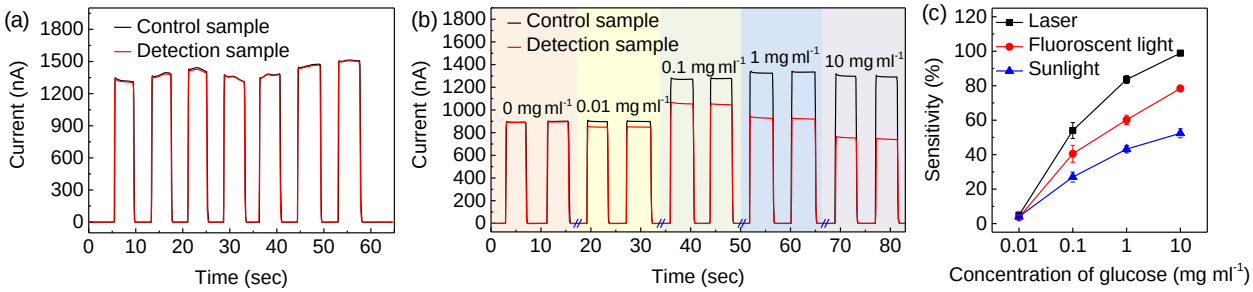

Figure 4. (a) Photocurrents of two self-powered biosensors under sunlight (sunny place). (b) Detection performance of the dual self-powered biosensors towards glucose in DI water in sunlight (five different graphs with differently colored backgrounds are joined). (c) Comparison of sensitivities of our devices under the three different light sources.

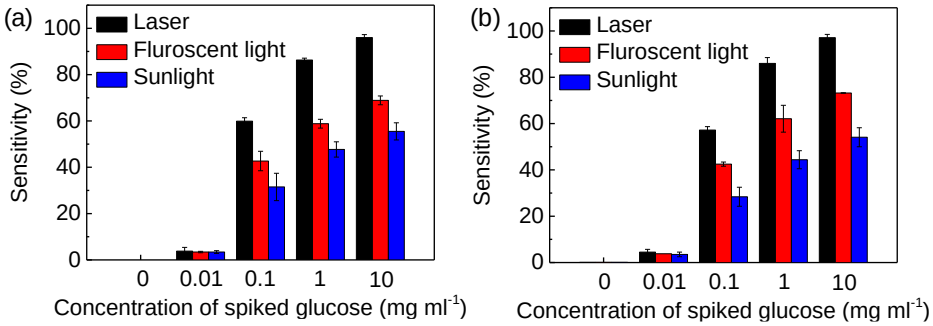

Figure 5. Sensitivities of the self-powered biosensors towards glucose in (a) pooled real human saliva and (b) pooled real human urine under the three different light sources.

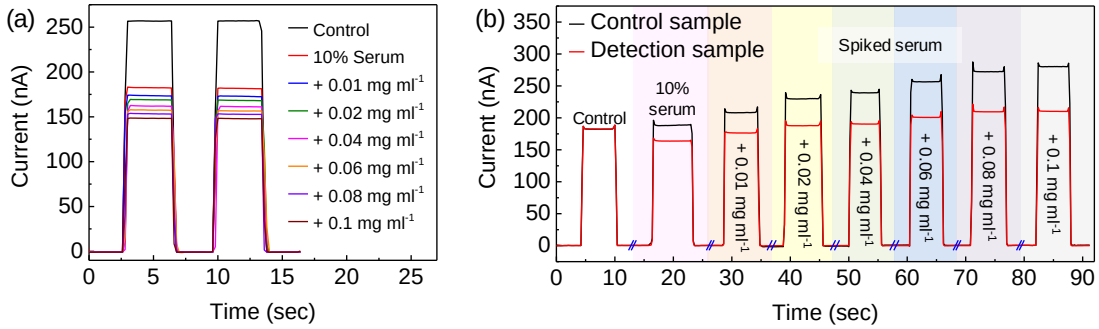

Figure 6. Sensitivities of the self-powered biosensors towards glucose in non-spiked and spiked human serum under (a) fluorescent light and (b) sunlight (eight different graphs with differently colored backgrounds are joined). Photocurrent measurement began 30 s after the target injection.

Table 1. Comparison of the performance of our devices and other self-powered glucose sensors reported in the literature

Method	Additional power supply	Matrix for glucose	Detection range (mM)	Reference
Electrochemistry	None	0.1 M PB, pH 7.0	1–80	(15)
Electrochemistry	None	0.1 M PBS	2–30	(30)
Electrochemistry	None	0.16 M PB, pH 7.0	0.2–1	(31)
Electrochemistry	None	Physiological glucose (w/ acetaminophen, ascorbic acid, uric acid, and lactic acid)	5–25	(32)
Electrochemistry	None	Not mentioned	1–5	(33)
Electrochemistry	None	0.1 M PBS, pH 7.0	10–50	(34)
Photoelectrochemistry	Need for light source	0.1 M PBS, pH 7.0	0.01–0.07	(22)
		Physiological glucose	3–8	
Photoelectrochemistry	Need for light source	0.1 M Tris-HCl buffer, pH 7.0	0.001–10	(23)
Photocurrent with colorimetric reaction	**None**	**Pooled human saliva and urine**	**0.055–55**	**This work**